J Solid State Electrochem (2016) 20:1075–1086
DOI 10.1007/s10008-015-2985-6

ORIGINAL PAPER

Electrode modification using nanocomposites of electropolymerised cobalt phthalocyanines supported on multiwalled carbon nanotubes

Stephen Nyoni[1] · **Philani Mashazi**[1] · **Tebello Nyokong**[1]

Received: 27 May 2015 / Revised: 13 July 2015 / Accepted: 20 July 2015 / Published online: 8 August 2015

Abstract A polymer of tetra(4)-(4,6-diaminopyrimidin-2-ylthio) phthalocyaninatocobalt(II) (CoPyPc) has been deposited over a multiwalled carbon nanotube (MWCNT) platform and its electrocatalytic properties investigated side by side with polymerized cobalt tetraamino phthalocyanine (CoTAPc). X-ray photoelectron spectroscopy, scanning electron microscopy and cyclic voltammetry studies were used for characterization of the prepared polymers of cobalt phthalocyanine derivatives and their nanocomposites. L-Cysteine was used as a test analyte for the electrocatalytic activity of the nanocomposites of polymerized cobalt phthalocyanines and multiwalled carbon nanotubes. The electrocatalytic activity of both polymerized cobalt phthalocyanines was found to be superior when polymerization was done on top of MWCNTs compared to bare glassy carbon electrode. A higher sensitivity for L-cysteine detection was obtained on CoTAPc compared to CoPyPc.

Keywords Electrocatalysis · L-Cysteine · Cobalt phthalocyanine · Electropolymerization · Multiwalled carbon nanotubes

Introduction

Metallophthalocyanine complexes (MPcs) are well-known electrocatalysts [1, 2]. Thin films of MPcs on solid electrode surfaces have been fabricated by different pathways including adsorption [1, 2], electropolymerization [3–8] and click chemistry [9] to name just a few. In this work, we fabricate an electrocatalytic platform in two steps: (i) firstly by drop-drying multiwalled carbon nanotubes (MWCNTs) on a glassy carbon electrode followed by (ii) electropolymerization of the cobalt phthalocyanine (CoPc) derivatives. The CoPc derivatives are the recently reported [10] tetra(4)-(4,6-diaminopyrimidin-2-ylthio) cobalt(II) phthalocyanine (CoPyPc) and the well-known cobalt tetraamino phthalocyanine (CoTAPc). We have reported on the electrocatalytic behavior of CoPyPc or CoTAPc in the presence of MWCNT when the CoPc derivatives and MWCNT are adsorbed onto glassy carbon electrode (GCE) [10, 11]. Adsorption is a fast and easy method. However, its limitation is that it is not often reproducible. Polymerization is more reliable and the thickness of the film can be controlled by the number of polymer cycles. Hence, this work reports on the polymerization of CoTAPc and CoPyPc (separately) onto MWCNT and evaluates their electrocatalytic activity. The polymerization of CoPyPc is reported in this work for the first time. CoPyPc has different polymerizable groups on the substituent, and we use X-ray photoelectron spectroscopy (XPS) to confirm the point of polymer formation on the CoPyPc molecule. A partial representation for polymerization of CoPc derivative is shown in Scheme 1 using CoPyPc as an example. We compare the electrocatalytic activities of the adsorbed and polymerized complexes. MWCNTs have been used as support systems to enhance electrocatalysis for MPcs and have good conductivity properties [12–15]. Electropolymerisation of CoTAPc on electrode surfaces is well known [3–8] but its electropolymerisation on a MWCNT platform for electrocatalysis has not been well studied. We show in this work that electropolymerizing CoTAPc on MWCNT improved electrocatalysis considerably compared to adsorption. We also compare the electrocatalytic behavior of CoTAPc

✉ Tebello Nyokong
t.nyokong@ru.ac.za

[1] Department of Chemistry, Rhodes University, P.O. box 94, Grahamstown, South Africa

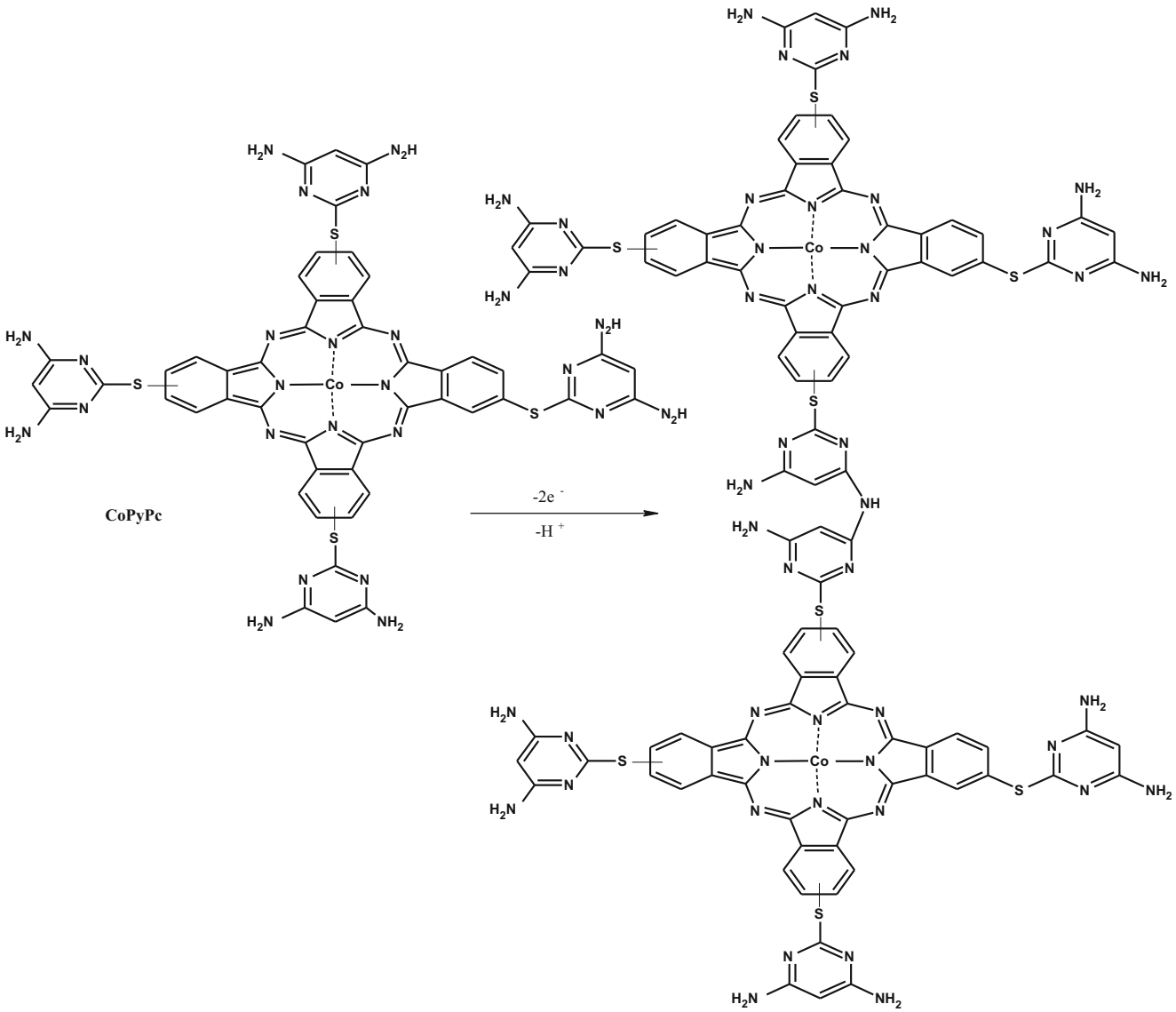

Scheme 1 Possible oxidative coupling for the formation of poly-CoPyPc. All terminal –NH_2 functional groups are capable of oxidative coupling to form straight and branched chains

polymerized on MWCNT with that of CoPyPc also polymerized on MWCNT. The cyclic voltammetry peaks for the Co^{III}/Co^{II} process (involved in electrocatalytic oxidation of L-cysteine) in polymerized CoTAPc are ill-resolved [16]. We employed CoPyPc in this work since it has additional amino groups (and has sulphur atoms); hence, it is expected that its oxidation will occur more readily and result in a more resolved Co^{III}/Co^{II} couple. However, CoPyPc might also have a more complex polymer due to the presence of a higher number of polymerizable groups compared to CoTAPc, resulting in different electrocatalytic properties.

The modified electrodes are employed for the detection of L-cysteine (as a test analyte), and the results are compared to when CoPc derivatives are adsorbed rather than polymerized. The effect of MWCNT on the electrocatalytic effect is evaluated. L-Cysteine was chosen since its high levels are associated with risks of vascular disease among many others [17]; hence, its detection is of importance. The oxidation of L-cysteine on polymerized CoTAPc (without MWCNTs) [4] or on CoTAPc mixed with MWCNTs [11] has been reported. This work shows that polymerizing CoTAPc on MWCNT improves electrocatalytic activity towards detection of L-cysteine.

Experimental

Materials

Dimethylformide (DMF), absolute ethanol, L-cysteine, buffer tablets, MWCNT, alumina and tetrabutylammonium

tetrafluoroborate ($TBABF_4$) were from Sigma Aldrich. CoPyPc [10] and CoTAPc [18] were synthesized according to literature.

Equipment

An Autolab Potentiostat PGSTAT30 equipped with GPES software version 4.9 was used for cyclic voltammetry studies. A three-electrode electrochemical cell comprising of a GCE (geometric area = 0.071 cm^2) as the working electrode, Ag|AgCl (3 M KCl) as reference electrode (for studies in aqueous media) and a platinum wire as the counter electrode was employed. An Ag wire pseudo reference electrode (Ag/AgCl) was employed for the electropolymerization of CoPc derivatives in DMF. BAS 100B electrochemical workstation was used for rotating disk electrode (RDE) voltammetry studies.

Scanning electron microscope (SEM) images were obtained using a JOEL JSM 840 scanning electron microscope. Glassy carbon plates (Goodfellow, UK) of 1 × 1 cm and 2 mm thick were used as substrates for SEM. X-ray photoelectron spectroscopy (XPS) analysis was done using an AXIS Ultra DLD, with Al (monochromatic) anode equipped with a charge neutraliser, supplied by Kratos Analytical. The following parameters were used: the emission was 10 mA, the anode (HT) was 15 kV and the operating pressure below 5×10^{-9} Torr. A hybrid lens was used and resolution to acquire scans was at 160 eV pass energy in slot mode. The centre used for the scans was at 520 eV with a width of 1205 eV, with steps at 1 eV and dwell time at 100 ms.

Electrode modification

The glassy carbon working electrode surface was polished using silicon carbide grinding paper (grit

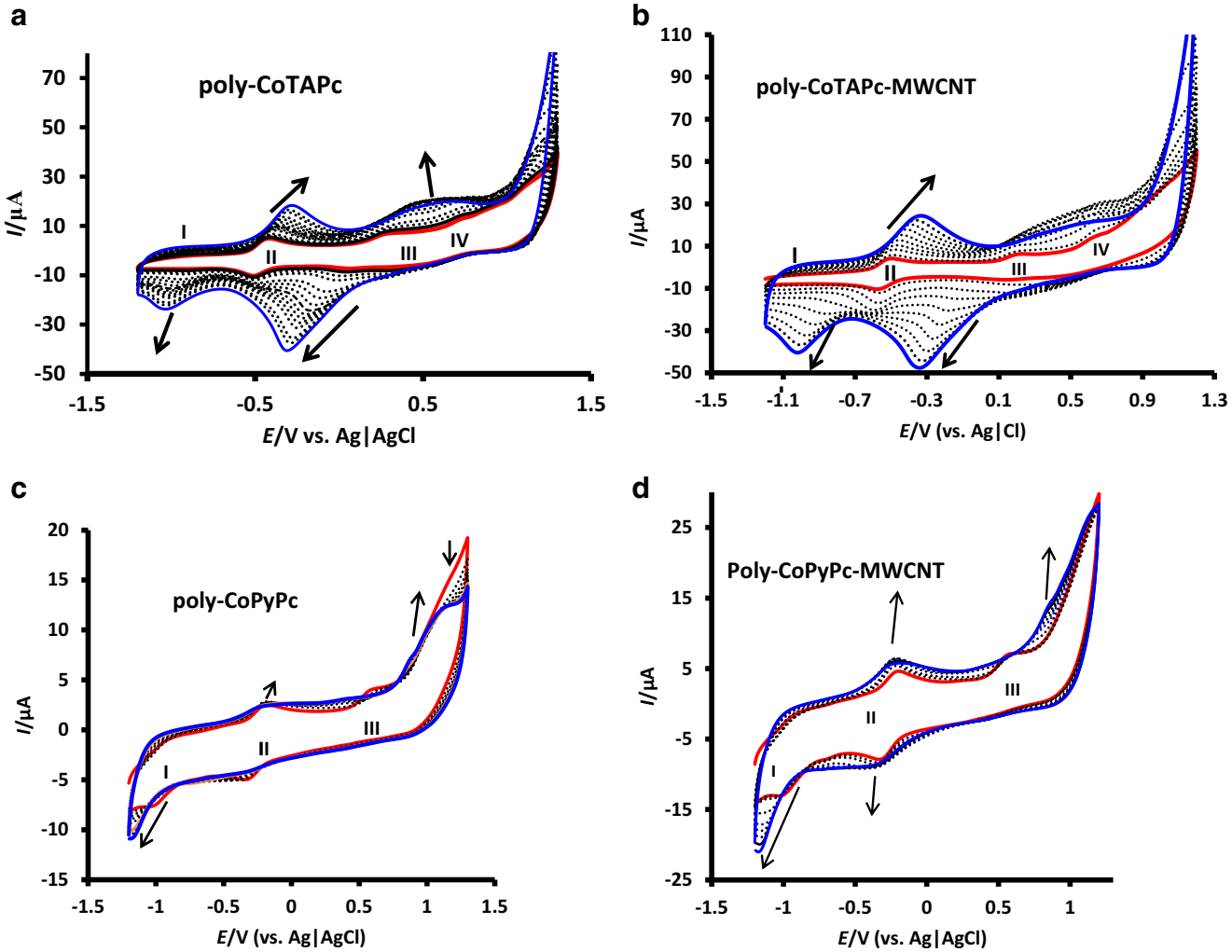

Fig. 1 Repetitive cyclic voltammograms of **a**, **b** 1 mM CoTAPc on GCE (**a**) and MWCNT-GCE (**b**). **c**, **d** 1 mM CoPyPc on GCE (**c**) and MWCNT-GCE (**d**). In DMF containing 0.1 M $TBABF_4$. Scan rate = 100 mV/s

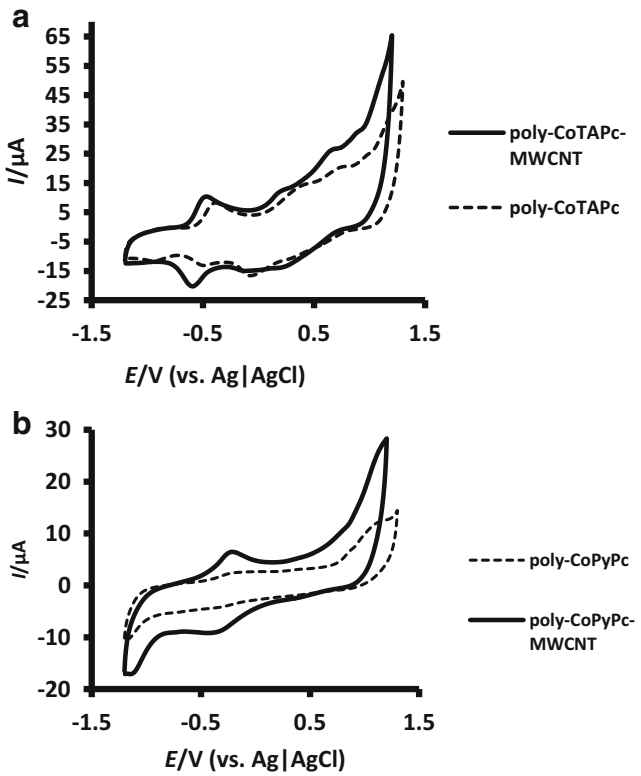

Fig. 2 Comparative cyclic voltammograms of the eight scan during the polymerization of 1 mM **a** CoTAPc and **b** CoPyPc on GCE and MWCNT. In DMF containing 0.1 M $TBABF_4$. Scan rate = 100 mV/s

1200) followed by polishing on a Buehler-felt pad using alumina (0.05 μm). Between each polishing step, brief sonication in absolute ethanol was used to remove any impurity. The electrode was then rinsed with Millipore water and dried under argon. The GCE was then modified with (i) poly-CoPyPc, (ii) poly-CoTAPc, (iii) poly-CoPyPc-MWCNT and (iv) poly-CoTAPc-MWCNT. Poly-CoPyPc-GCE and poly-CoTAPc-CGE were prepared by repetitive cyclic voltammetry scanning of the bare GCE in their respective 1×10^{-3} M solutions prepared in DMF containing 0.1 M $TBABF_4$ electrolyte. Poly-CoPyPc-MWCNT-GCE and poly-CoTAPc-MWCNT-GCE were prepared in two stages; (i) 0.5 μL MWCNT (1 mg per 1 mL in DMF) was drop-dried onto the GCE followed by (ii) repetitive cyclic voltammetry scanning of the MWCNT modified GCE in 1.0×10^{-3} M of each CoPc derivative solution. After the repetitive scanning process, the electrode was rinsed with dry DMF and dried under argon before each use. RDE experiments for kinetic studies were done in 8 mM L-cysteine. Experiments were also performed where CoPyPc (a drop of 1.0×10^{-3} M solution) was added to the GCE followed by drying, represented as adsorbed-CoPyPc-GCE. CoPyPc (1 mL of 0.001 M) was also mixed with 1 mL MWCNT (1 mg per 1 mL in DMF), and 0.5 μL of the mixture was added to the electrode followed by drying, represented as mixed-

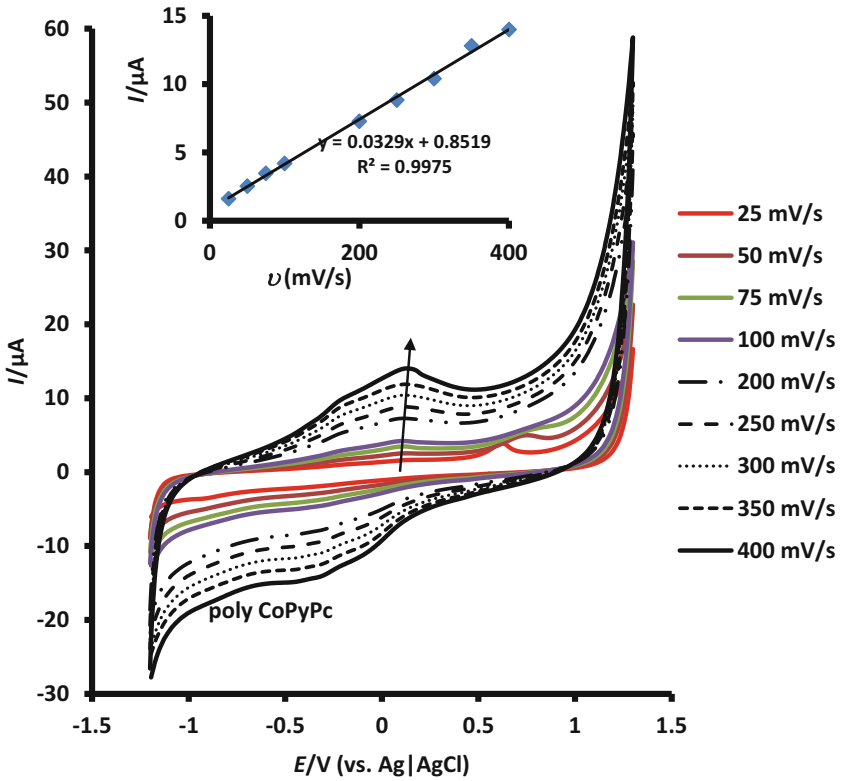

Fig. 3 Cyclic voltammograms of poly-CoPyPc thin film on bare GCE in pH 4 buffer solution, (*inset* plot of I_p vs. υ and the *arrow* shows where I_p were taken)

Table 1 Rate constants for L-cysteine oxidation and surface coverage for the modified electrodes

Electrode type	Rate constant, k (cm s^{-1}) For L-cysteine detection	Surface coverage, Γ (mol cm^{-2})
poly-CoTAPc-GCE	6.16×10^{-4}	2.69×10^{-9}
poly-CoTAPc-MWCNT-GCE	1.54×10^{-3}	2.33×10^{-9}
poly-CoPyPc-GCE	2.66×10^{-4}	3.04×10^{-10}
poly-CoPyPc-MWCNT-GCE	4.33×10^{-4}	3.49×10^{-10}

CoPyPc-MWCNT-GCE. The detection of L-cysteine on adsorbed-CoTAPc-GCE and mixed-CoTAPc-MWCNT-GCE has been reported before [11].

Results and discussion

Electropolymerization of poly-CoPc derivatives on bare and MWCNT-GCE

The electropolymerization of CoTAPc or CoPyPc on GCE or MWCNT-GCE was achieved through repetitive potential scanning in 1×10^{-3} mol L^{-1} of their respective monomeric phthalocyanines, in freshly distilled DMF containing 0.1 M $TBABF_4$ supporting electrolyte (Fig. 1a–d). The polymerization of CoTAPc on bulk carbon electrodes is well known [3–8] (Fig. 1a). The cyclic voltammogram changes observed during polymerization of CoTAPc in Fig. 1a are similar to those reported in literature [7, 19] but the peaks are more resolved in the current work. Figure 1b shows the electropolymerization of CoTAPc on adsorbed MWCNT. Figure 1c, d shows the electropolymerization of CoPyPc on GCE and on MWCNT-GCE, respectively. During polymerisation process, it was observed in all cases that the first scans (red lines) were different from subsequent scans, an indication of polymer formation. Furthermore, subsequent scans exhibited increasing currents, and this confirms the growth and development of better conducting polymeric species on electrode surface. Figure 2a, b summarizes the CVs of the polymeric forms in the presence and absence of MWCNT. Only scans number 8 were plotted for comparison in Fig. 2. Figure 2 shows an increase in conducting properties when the polymeric forms of both MPc derivatives were formed on MWCNT, hence confirming that MWCNT promote electron transfer. There was a larger current increase during the polymerization of CoTAPc compared to CoPyPc on both GCE and MWCNTs, suggesting better conductivity for the former. Polymerization was continued until there was no further increase in current; the resulting electrode was employed for electrocatalysis.

Process II in Fig. 1 may be assigned to $Co^{II/I}$ redox couple while process III is likely to correspond to $Co^{III/II}$ redox couple in comparison with literature [16, 19–21]. Process III is not well resolved as has been observed before [16]. Increasing the number of scans for polymer formation was reported not to improve resolution of the process III peaks [16]. The Co^{III}/Co^{II} process III was more resolved for CoPyPc compared to CoTAPc, but only during the first scan, there after the peaks were weaker probably due the nature of the polymer formed.

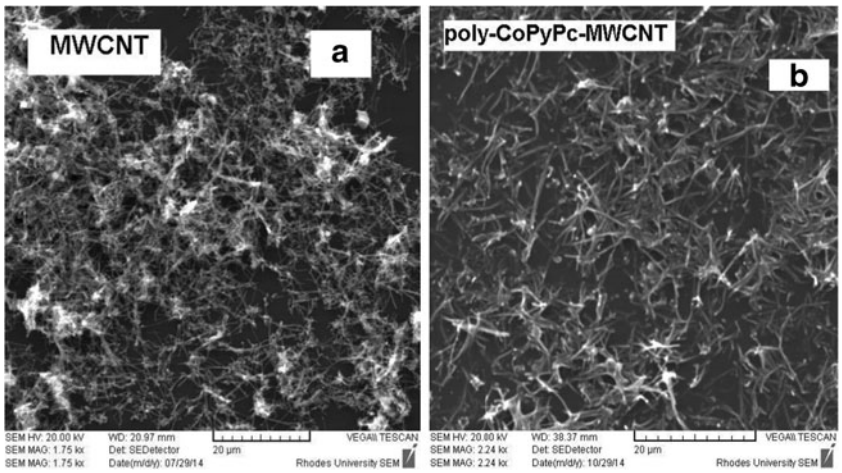

Fig. 4 SEM images (on glassy carbon plates) of MWCNT before (**a**) and after polymerisation with CoPyPc (**b**)

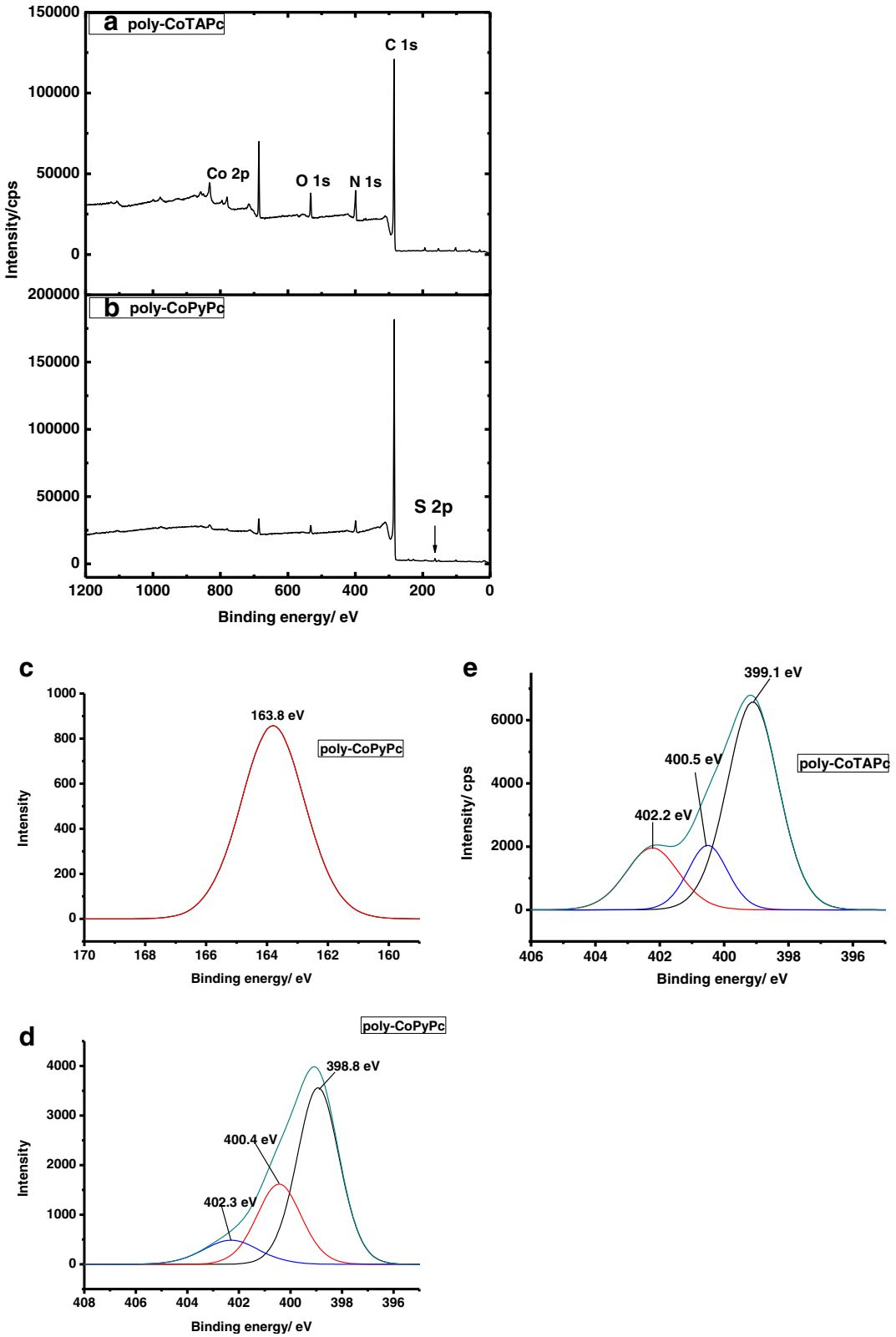

Fig. 5 Wide scan XPS spectra for poly-CoTAPc **a** poly-CoPyPc **b.** High-resolution deconvoluted XPS peaks for S 2p **c** and N 1s for poly-CoPyPc (**d**), and N 1 s for poly-CoTAPc (**e**). All on MWCNT-modified glassy carbon plates

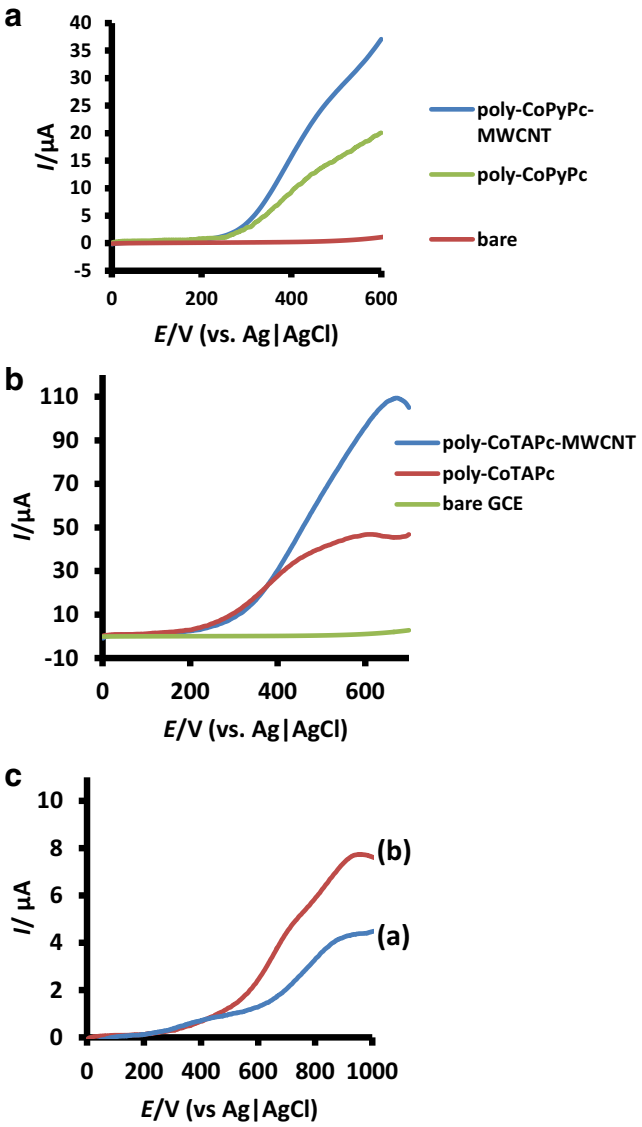

Fig. 6 Comparative RDE voltammograms for 8 mM L-cysteine (in pH 4 buffer) at **a** bare GCE, poly-CoPyPc and poly-CoPyPc-MWCNT surfaces, **b** bare GCE, poly-CoTAPc, and poly-CoTAPc-MWCNT surfaces and **c** adsorbed-CoPyPc (*a*) and mixed- CoPyPc-MWCNT (*b*). Scan rate = 10 mV/s, rotational speed 400 rpm for (**a**) and (**b**) and 1000 rpm for (**c**)

The peaks near 1 V are associated with the oxidation of the amino group [22]. The rest of the processes are phthalocynanine ring-based.

Characterization of modified electrodes

Cyclic voltammetry (CV)

CVs were run for each modified electrode system at varying scan rates in pH 4 buffer system (Fig. 3, using CoPyPc as an example).

The active electrode area (A) was obtained through the Randles-Sevcik (Eq. 1) [23] and used to calculate the surface coverage.

$$I_p = 2.69 \times 10^5 nACD^{\frac{1}{2}}\nu^{\frac{1}{2}}, \quad (1)$$

where I_p = current maximum in amps, A = electrode area in cm^2, n = number of electrons transferred in the redox process, C = concentration in mol/cm^3, D = diffusion coefficient in cm^2/s and υ = scan rate in V/s. $[Fe(CN)_6]^{3-/4-}$ redox system was employed with a diffusion coefficient of 7.6×10^{-6} cm^2 s^{-1} [24], concentration = 1 mM and n = 1.

The data obtained Fig. 3 was used to estimate the surface coverages (Γ) using Eq. 2 [25, 26].

$$I_p = \frac{n^2 F^2 \nu A \Gamma}{4RT} \quad (2)$$

where I_p, n, F, v, A and Γ are redox peak current, number of electrons, Faraday's constant, scan rate, surface area (determined above) and surface coverage of the catalyst, respectively. The slopes from the plots of Ip vs. υ (Fig. 3, inset) were then used to calculate surface coverages. Values are summarised in Table 1. The Γ values for poly-CoTAPc and poly-CoTAPc-MWCNT are higher than for poly-CoPyPc and poly-CoPyPc-MWCNT. This can be attributed to the different functionalities between the substituent groups which influence different pathways for polymer formation. However, there was a small difference in Γ values between poly-MPcs and their respective nanocomposites (poly-MPc-MWCNT). This indicates that the MWCNTs do not have a strong influence on polymer formation. Γ values for all the catalysts are greater than 1×10^{-10} mol cm^{-2} which is expected for a monolayer of a Pc molecule lying flat on the electrode surface [27, 28]. This might be expected for Pcs alone, since the polymer formed may be more than a monolayer and for Pc-MWCNT because the polymer formation is on a MWCNT layer and not on a flat surface.

Scanning electron microscopy studies

Some structural changes of the MWCNT were observed after polymerisation (Fig. 4). The images of MWCNT show a porous structure before polymerization of CoPyPc. There was more interconnection of the CNTs following polymerization, which is further confirmation of successful polymerization to form the polymer nanocomposite. This may be a result of both straight and side polymer chains being produced during repetitive cyclisation of the CoPyPc monomer solution at a MWCNT modified GCE surface. The SEM image for poly-CoTAPc was similar to that of poly-CoPyPc.

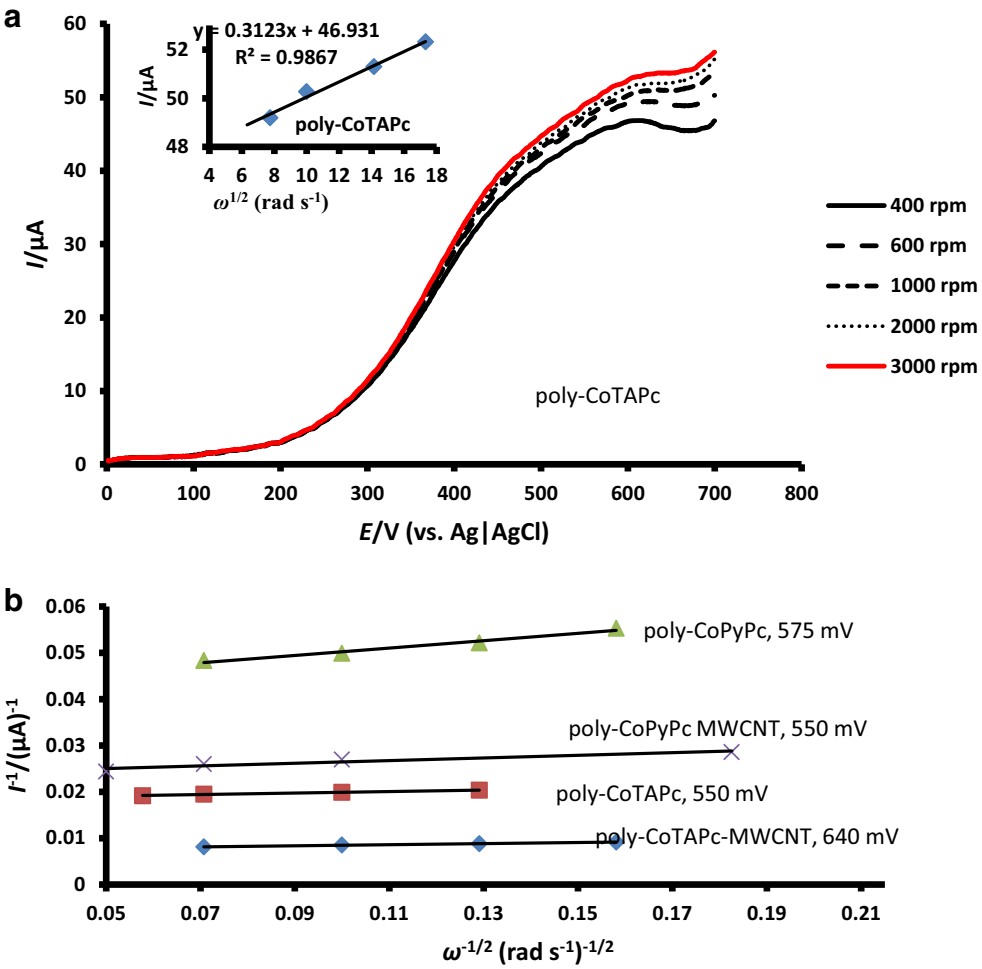

Fig. 7 **a** RDE voltammograms of 8 mM L-cysteine (in pH 4 buffer) on poly-CoTAPc at different rotation rates. Scan rate = 10 mV/s, *inset* Levich plot for the film. **b** Koutecky-Levich plots for the electrooxidation of 8 mM L-cysteine in pH 4 buffer on polymer films

XPS characterization

XPS analysis was used to check the possible polymerization points on CoPyPc for the formation of poly-CoPyPc. Figure 5a, b shows the wide scan XPS for poly-CoTAPc and poly-CoPyPc, respectively. The peaks due to N, C and Co are observed for both complexes as expected. The observed oxygen peak is likely to be a result of adsorbed oxygen from air since no C–O functionalities are expected from the chemical structure of the Pc alone depicted in Scheme 1. We also observed an intense fluoride (F 1s) peak at around 690 eV due to the supporting electrolyte ($TBABF_4$) used during the electropolymerization of the two complexes onto glassy carbon electrodes. The high-resolution scans were also conducted and deconvoluted to get more information on the identified elements and to investigate different components with their functionalities/chemical environments within the polymers. Figure 5c shows the deconvoluted spectrum of S $2p_{3/2}$ for poly-CoPyPc. Only one peak was observed at 163.8 eV. One S 2p peak has been reported before [29]. This has been assigned to sulphur in a chemical environment of C–S–C, according to the NIST Standard Reference Database [30, 31]. This agrees well with the structure of CoPyPc shown in Scheme 1, in which the sulphur is the bridging atom between the MPc ring and the substituent and not with a neighbouring MPc monomer ring. The N 1s spectrum for poly-CoPyPc (Fig. 5d) shows three main peaks after deconvolution, implying the existence of nitrogen in three different chemical environments in the polymer. These can be assigned to C–N=C/C–N–C (398.8 eV) nitrogens mainly from MPc rings and the other nitrogens involved in the polymerization process as the interconnectors between monomeric MPcs units as depicted in Scheme 1. Peaks at 400.4 and 402.3 eV can be assigned to $–N^+H$ and $=N^+H$, respectively. These are oxidized amine groups which have not taken part in polymer formation, and the presence of the positive charge shifts their binding energies to more positive values than $–NH_2$ (~399.1 eV [32]). Similar spectra were obtained for poly-CoTAPc (Fig. 5e) after deconvolution, indicating the same electropolymerisation

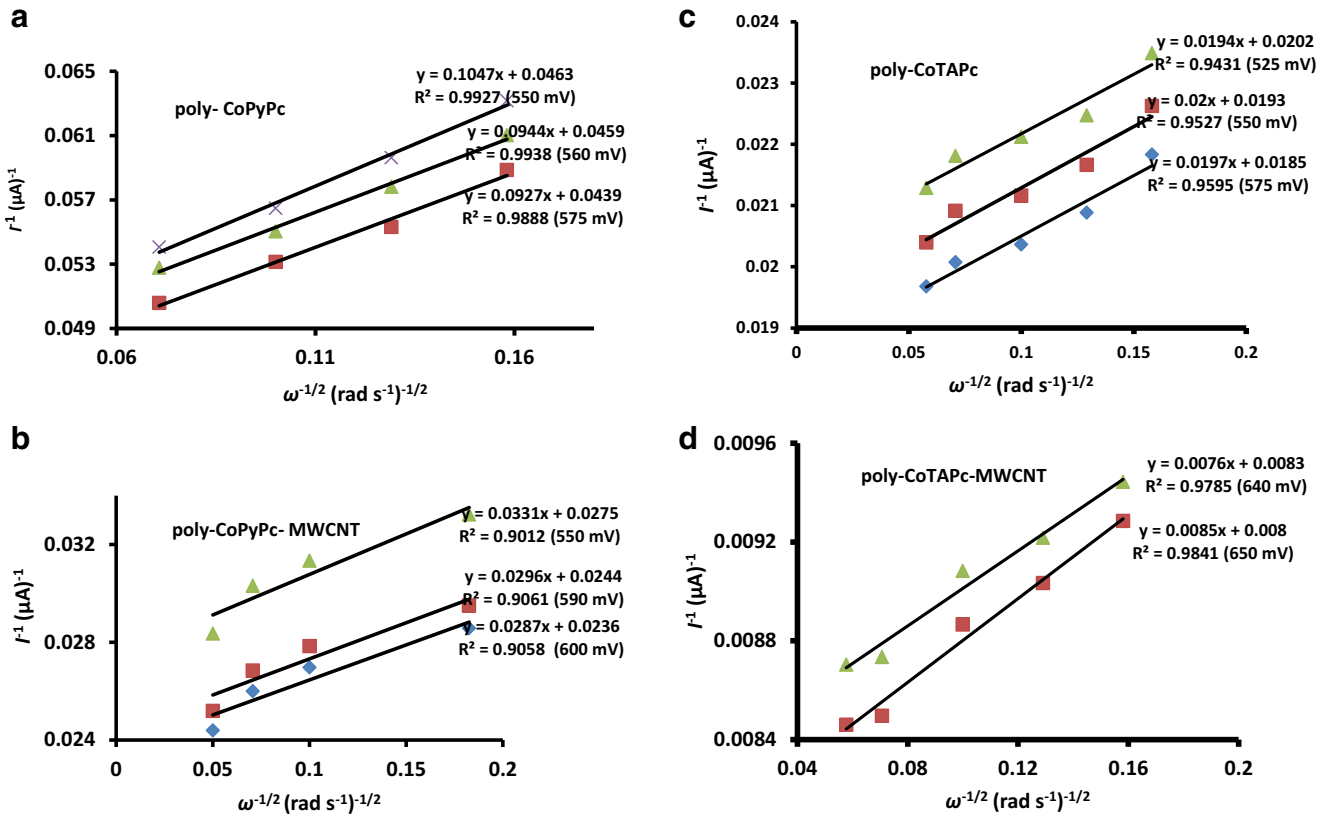

Fig. 8 Plots of I^{-1} vs. $\omega^{-1/2}$ from RDE voltammograms of 8 mM L-cysteine (in pH 4 buffer) on **a** poly-CoPyPc, **b** poly-CoPyPc-MWCNT, **c** poly-CoTAPc and **d** poly-CoTAPc-MWCNT at different rotational speeds at the specified potentials values

mechanism for the two polymeric forms. This is further evidence supporting that sulphur is not participating in the growth of conducting polymer films.

Electrocatalytic oxidation of L-cysteine

RDE kinetic studies for electrooxidation of L-cysteine

The kinetics of electrooxidation of L-cysteine were performed by hydrodynamic RDE voltammetry technique in 8 mM L-cysteine. Figure 6a compares RDE voltamograms of bare GCE, poly-CoPyPc and poly-CoPyPc-MWCNT. There was no electrooxidation of L-cysteine in pH 4 buffer on a bare GCE within the potential window used in Fig. 6.

There was a distinct and remarkable activity observed from poly-CoPyPc relative to the bare GCE. It was also interesting to note that the poly-CoPyPc-MWCNT nanocomposite gave much higher currents than poly-CoPyPc for the electrooxidation of L-cysteine, indicating the importance of polymerizing the MPc over a MWCNT platform than on a bare GCE. The same behaviour where currents are higher in the presence of MWCNT was also observed for poly-CoTAPc-MWCNT compared to poly-CoTAPc (Fig. 6b). For adsorbed-CoPyPc and mixed-CoTAPc-MWCNT, much lower currents for L-cysteine detection were obtained even at a higher rotation speed (Fig. 6c), showing the polymerization results in better results.

RDE voltammograms for the electrooxidation of L-cysteine were also recorded at varying rotational speeds for all the four electrocatalysts (Fig. 7) (using poly-CoTAPc as an example). Figure 7 shows that the process of L-cysteine electro-oxidation is largely under the kinetic control even at relatively high potentials.

The inset in Fig. 7a shows the Levich plots (I_L vs. $\omega^{1/2}$) obtained from the Levich Eq. 3 [23].

$$I_{\mathrm{L}} = 0.62nFAD^{\frac{2}{3}}\omega^{\frac{1}{2}}\nu^{\frac{-1}{6}}C, \tag{3}$$

where n, F, A, D, ω, υ, and C represent number of electrons, Faraday's constant, effective surface area of the electrode in cm^2, diffusion coefficient in $cm^2\ s^{-1}$, rotational speed in rad s^{-1}, kinematic viscosity in $cm^2\ s^{-1}$ and bulk concentration of the analyte in mol cm^{-3}. The plot shows the expected linear dependence of the limiting currents against square root of rotational speed predicted by the Levich equation, indicative of diffusion controlled mass transport. Further kinetic details of the electrooxidation of L-cysteine on these catalysts were derived from the Koutecky-Levich Eq. 4 [23].

$$\frac{1}{I} = \frac{1}{\mathrm{nFAkC}} + \frac{1}{0.62nFA\nu^{\frac{-1}{6}}D^{\frac{2}{3}}\omega^{\frac{1}{2}}}, \tag{4}$$

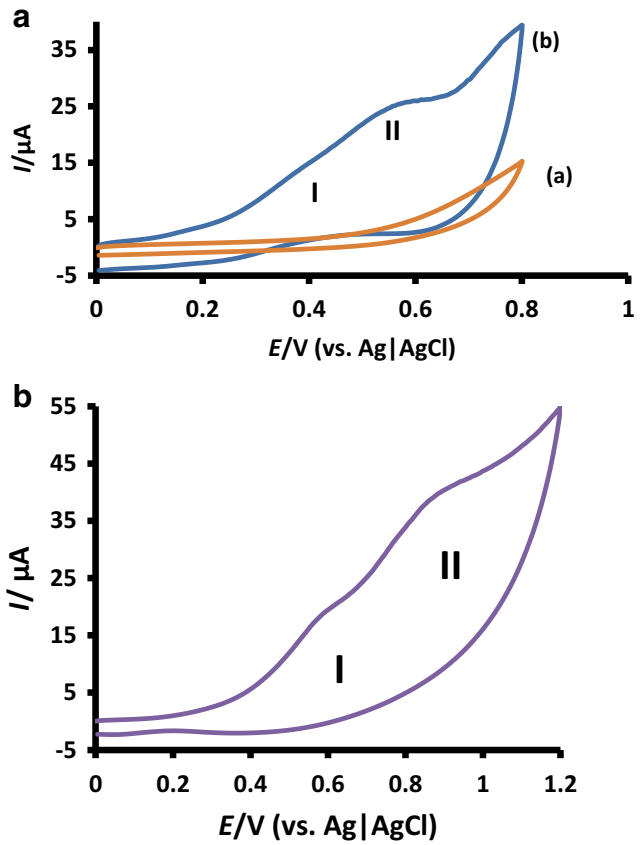

Fig. 9 Comparative cyclic voltammograms of 8 mM L-cysteine in pH 4 buffer at a **a** bare GCE (*a*) and poly-CoPyPc-MWCNT-GCE (*b*), **b** for electrode modified with mixed CoPyPc-MWCNTs. Scan rate = 100 mV/s

where k is the reaction rate constant in cm s^{-1} and other quantities have their scientific meaning as defined above. The intercepts of the Koutecky-Levich plots ($I^{-1} vs. \omega^{\frac{-1}{2}}$) shown in Fig. 7b were used for determination of the kinetic reaction rate constants (summarised in Table 1) for the electrooxidation of L-cysteine at the polymer film surfaces.

The rate constant values show that the rate of electrooxidation of L-cysteine was greatly improved when the polymers were formed on MWCNT, making nanocomposite electrocatalysis more favourable than individual Pc polymers. The higher k values for poly-CoTAPc and poly-CoTAPc-MWCNT are consistent with surface coverage data. The observed better current responses for poly-CoTAPc and poly-CoTAPc-MWCNT can also be attributed to higher polymer porosity than for poly-CoPyPc, allowing for more active sites to be exposed to the analyte. Reaction kinetics in terms of the order of reaction with respect to the test analyte was obtained from the plot of I^{-1} vs. $\omega^{-1/2}$ (Fig. 8a–d), where I is the current taken from the rising part the RDE voltammograms in Fig. 7a at the specified potentials shown in brackets in Fig. 8a–d. Parallel lines with almost constant slopes were obtained, illustrating a first-order reaction with respect to L-cysteine electrooxidation.

Cyclic voltammetric studies for the detection of L-cysteine

Figure 9a (using poly-CoPyPc-MWCNT as an example) shows the cyclic voltammograms of L-cycteine in pH 4 buffer solutions on bare GCE and poly-CoPyPc-MWCNT, while Fig. 9b shows the voltammograms on electrodes modified with mixed-CoPyPc-MWCNTs. The individual polymers of CoPyPc and CoTAPc were not investigated further since they proved to be less electroactive than their respective polymeric nanocomposites. No current responses were obtained with the bare GCE within this potential window in pH 4 buffer, Fig. 9a. Irreversible oxidation peaks were observed on film of nanocomposites. The redox peaks labelled I are associated with Co^{III}/Co^{II} in Fig. 9a. The processes labelled II in Fig. 9 are due to L-cysteine oxidation. This was confirmed the increase in the currents of process II with increase in L-cysteine concentration (figure not shown). The peaks for L-cysteine oxidation on poly-CoTAPc-MWCNT and poly-CoPyPc-MWCNT were observed at approximately 0.40 and 0.55 V, respectively. The potential for the oxidation of L-cysteine in pH 4 buffer on mixed-CoTAPc-MWCNT was reported to be 0.63 V [11] and 0.83 V for mixed-CoPyPc-MWCNTs (Fig. 9b). Both potentials are much higher than obtained here for the polymerization of CoTAPc or CoPyPc onto MWCNTs. Thus, nanocomposites involving polymeric MPcs have better electrocatalytic properties than monomeric MPcs films for L-cysteine oxidation in terms of oxidation peak potential.

The electrocatalytic oxidation peaks in both cases were observed in the potential region close to the CoIII/II process, implying that electrocatalysis is mediated by this redox couple. The mechanism will be as proposed before [33] in acid media. The cyclic voltammetry peaks are not well resolved; hence, chronoamperometry will be employed below.

Chronoamperometry studies

Chronoamperometry technique was used to gain more information on analytical parameters such as limit of detection (LOD), sensitivity and stability. This technique was chosen since it gives a better signal-to-noise ratio than other amperometric techniques [23].

The chronoamperometry steps produced upon addition of 0.03 mM L-cysteine aliquots are shown in Fig. 10a. Poly-CoTAPc-MWCNT nanocomposite film showed better catalytic current responses than poly-CoPyPc-MWCNT nanocomposite film. The differences in the rate of increase of catalytic currents with time are clearly shown by slopes of the plots of cumulative step currents against time (Fig. 10a, inset). Furthermore, the catalytic step currents remain higher and stable for poly-CoTAPc-MWCNT nanocomposite film compared to poly-CoPyPc-MWCNT. Stability tests were done by performing ten chronoamperometry scans in 0.27 mM L-

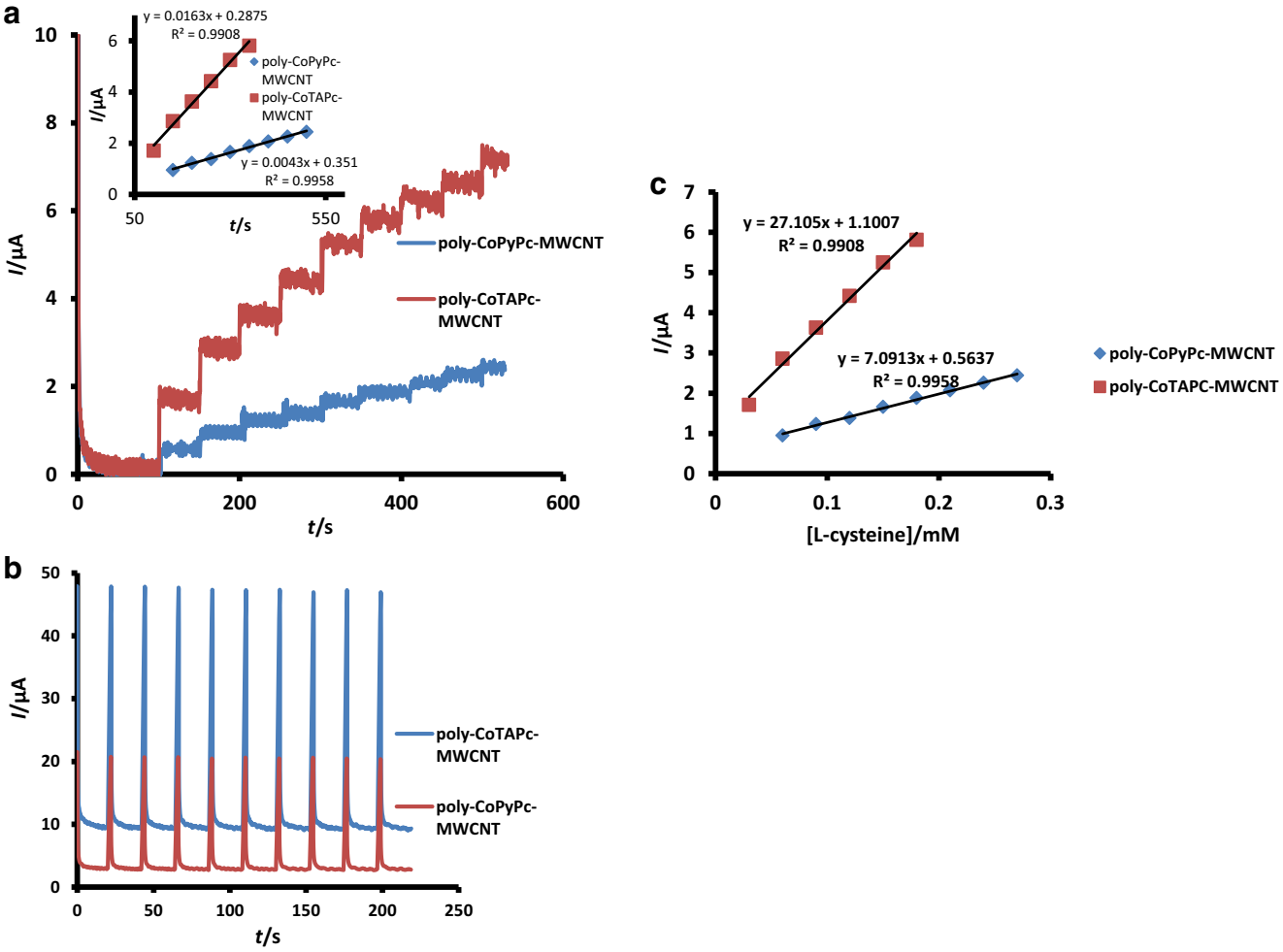

Fig. 10 **a** Electrooxidation chronoamperogram steps at poly-CoPyPc-MWCNT and poly-CoTAPc-MWCNT thin films after successive additions of aliquots of L-cysteine in pH 4 buffer. **b** Repetitive chronoamperommograms in 0.27 mM L-cysteine in pH 4 buffer using poly-CoPyPc-MWCNT (*red*) and poly-CoTAPc-MWCNT (*blue*) thin films. **c** Plots of cumulative electrooxidative currents after addition of aliquots of 0.03 mM L-cysteine using poly-CoPyPc-MWCNT and poly-CoTAPc-MWCNT thin films

cysteine (Fig. 10b). Both surfaces showed very stable catalytic currents for the ten chronoamperometry scans, however, poly-CoTAPc-MWCNT nanocomposite film gave higher catalytic currents as observed in Fig. 10a. From the plots of current vs. concentration of L-cysteine (Fig. 10c), sensitivity and LOD parameters were derived. Under these hydrodynamic conditions, poly-CoTAPc-MWCNT film was more sensitive (27.11 μA/mM L-cysteine) than poly-CoPyPc-MWCNT film (7.09 μA/mM L-cysteine). The LOD of detection for poly-CoTAPc-MWCNT and poly-CoPyPc-MWCNT were found (using the 3σ notation) to be 1.74×10^{-8} M and 3.55×10^{-8} M, respectively. These values are well below the LOD observed on monomeric CoTAPc mixed with MWCNT (2.8×10^{-7} M [11]). Also the LOD for mixed CoPyPc-MWCNTs is less favourable than for poly-CoPyPc (Table 2). These observations imply that polymeric MPcs are better candidates for fabrication of MPc-MWCNT nanocomposite electrocatalysts than monomeric derivatives. Thus, even though poly-CoPyPc is

Table 2 Comparative LODs for the electrocatalysed oxidation of L-cysteine using different catalytic systems

Electrode	pH	LOD	Ref.
MWCNT-FeTsPc (mixed)-GCE	pH 7	1 μM	[30]
CoPc-carbon paste	pH 2.4		[31]
CoOHETPc-SAM-Au	pH 4	0.52 μM	[32]
FeOHETPc-SAM-Au	pH 4	0.52 μM	[32]
Mixed-CoTAPc-MWCNT-GCE	pH 4	0.28 μM	[9]
Mixed-CoPyPc-MWCNT-GCE	pH 4	0.296 μM	This work
poly-CoPyPc-MWCNT	pH 4	0.036 μM	This work
poly-CoTAPc-MWCNT	pH 4	0.017 μM	This work

OHETPc octa(hydroxyethylthio) phthalocyanine, *SAM* self-assembled monolayer

not as sensitive as poly-CoTAPc for L-cysteine detection, the LOD for L-cysteine oxidation is lower than that for the commonly used monomeric CoTAPc and for other electrodes modified with MPc complexes (Table 2) [11, 34–36].

The higher LOD for L-cysteine on poly-CoPyPc compared to poly-CoTAPc could be related to the different types of polymers formed, with the former having more polymerizable NH_2 groups, hence a more complex polymer. It is also interesting to note that the levels of L-cysteine in human beings ~250 μM [17] are far much higher than the LODs reported here. This makes clinical applications at levels lower than 250 μM accessible at these thin polymer nanocomposite films.

Conclusions

Cobalt metallophthalocyanine derivatives were electropolymerised on both the bare GCE and MWCNT-GCE to form polymerised electrocatalytic films. Electrocatalytic performance was evaluated for the polymer films, and we found out that the polymer films behaved better when supported on MWCNT than on bare GCE. Improved sensitivity, kinetic rate constants and lower LODs were obtained for the nanocomposites. In terms of limit of detection, the polymer of CoPyPc performs better than other MPc-based electrodes, but has less sensitivity compared to poly-CoTAPc.

Acknowledgments This work was supported by the Department of Science and Technology (DST) and National Research Foundation (NRF), South Africa, through DST/NRF Research Chairs Initiative for Professor of Medicinal Chemistry and Nanotechnology (IUD 62620) as well as Rhodes University and DST/Mintek Nanotechnology Innovation Centre (NIC)—Sensors, South Africa. SN thanks African laser centre for a scholarship.

References

1. Lalande G, Cote R, Tamizhmani G, Guay D, Dodelet JP, Dignard-Bailey L, Weng LT, Bertran P (1995) Electrochim Acta 40:2635–2646
2. Nyokong T (2006) Electrodes modified with monomeric M-N4 catalysts for the detection of environmentally important molecules. In: Zagal JH, Bedioui F, Dodelet J-P (eds) N4-macrocyclic metal complexes. Springer, New York, p. 315
3. Xu F, Li H, Cross SJ, Guarr TF (1994) J Electroanal Chem 368:221–225
4. Qi X, Baldwin RP RP (1996) J Electrochem Soc 143:1283–1287
5. Fan J-P, Zhang X-M, Ying M (2010) S Afr J Chem 63:145–151
6. Brown KL, Shaw J, Ambrose M, Mattola HA (2002) Microchem J 72:285–298
7. Griveau S, Albin V, Pauporté T, Zagal JH, Bedioui F (2002) J Mater Chem 12:225–232
8. Qi X, Baldwin RP, Li H, Guarr TF (1991) Electroanalysis 3:119–124
9. Coates M, Nyokong T (2012) J Electroanal Chem 687:111–116
10. Nyoni S, Nyokong T (2014) Electroanalysis 26:2261–2272
11. Nyoni S, Mugadza T, Nyokong T (2014) Electrochim Acta 128:32–40
12. Kruusenberg I, Matisen L, Tammeveski K (2013) Int J Electrochem Sci 8:1057–1066
13. Songa H, Qiua X, Li F (2008) Electrochim Acta 53:3708–3713
14. Guo D-J, Jing Z-H (2010) J Power Sources 195:3802–3805
15. Jiang Z, Yu X, Jiang Z-J, Menga Y, Shi Y (2009) J Mater Chem 19:6720–6726
16. Griveau S, Pavez J, Zagal JH, Bedioui F (2001) J Electroanal Chem 497:75–83
17. El-Khairy L, Ueland PM, Refsum H, Graham IM, Vollse SE (2001) Circulation 103:2544–2449
18. Somashekarappa MP, Keshavanyya J, Sampath S (2002) Pure Appl Chem 74:1609–1620
19. Tse Y, Janda P, Lam H, Zhang JJ, Pietro WJ, Lever ABP (1997) J Porphyrins Phthalocyanines 1:3–16
20. Sivanesan A, John S (2008) Langmuir 24:2186–2196
21. Sivanesan A, John S (2009) Electrochim Acta 54:7458–7463
22. Ramirez G, Trollund E, Isaacs M, Armijo F, Zagal J, Costamagna J, Aguirre MJ (2002) Electroanalysis 14:540–545
23. Bard AJ, Faulkner LR (2000) Electrochemical methods: fundamentals and applications, 2nd edn. Wiley, New York
24. Gooding J, Praig V, Hall E (1998) Anal Chem 70:2396–2402
25. Eckermann AL, Feld DJ, Shaw JA, Meade TJ (2010) Coord Chem Rev 254:1769–1802
26. Fotouhi L, Fatollahzadeh M, Heravi MM (2012) Int J Electrochem Scie 7:3919–3928
27. Li Z, Lieberman M, Hill W (2001) Langmuir 17:4887–4894
28. Zagal JH, Gulppi MA, Depretz C, Lelievre D (1999) J Porphyrins Phthalocyanines 3:355–363
29. Huang J, Hemminger JC (1993) J Am Chem Soc 115:3342–3343
30. NIST Standard Reference Database 20, Version 3.4 (web version) (http://srdata.nist.gov/xps/) (2003)
31. Smart RSC, Skinner WM, Gerson AR (1999) Surf Interface Anal 28:101–105
32. Gengenbach TR, Chatelier RC, Griesser HJ (1996) Surf Interface Anal 24:611–619
33. Maree S, Nyokong T (2000) J Electroanal Chem 492:120–127
34. Devasenathipathy R, Mani V, Chen AM, Kohilarani K, Ramaraj S (2015) Int J Electrochem Sci 10:682–690
35. Khaloo SS, Amini MK, Tangestaninejad S, Shahrokhian S, Kia R (2004) J Iran Chem Soc 1:128–135
36. Ozoemena KI, Nyokong T, Westbroek P (2003) Electroanalysis 14:1762–1770